radicals; analogous products were observed by ESR spectrometry in the oxidation of kojic acid by Ce(IV).[24] We assume that such radicals are formed in the reduction of Np(VI) by HK. Such phenoxy radicals would be unstable because the nonbonding orbital of the oxygen atom does not overlap with the π-bonding orbitals of the ring. There may be ring cleavage in the subsequent reaction of the phenoxy radical of kojic acid.

The empirical rate law, eq 1, as well as the linear plot of the ln (k/T) vs $1/T$ data, excludes a mechanism consisting either of successive steps or of two or more competing parallel pathways with transition states of different composition. The inverse hydrogen ion dependence on the rate indicates the existence of an equilibrium preceding the rate-limiting step with the hydrogen ion produced as a byproduct in this equilibrium. Such a deprotonation is most likely associated with formation of kojate anions from kojic acid. The effect of ionic strength is consistent with the interaction of the kojate anions with NpO_2^{2+} to form the activated complex. These considerations lead to the mechanism

$$HK \overset{K_a}{\rightleftharpoons} H^+ + K^- \quad (2)$$

$$NpO_2^{2+} + K^- \overset{\beta_1}{\rightleftharpoons} [NpO_2K^+] \rightleftharpoons [NpO_2K^+]^* \quad (3)$$

$$[NpO_2K^+]^* \xrightarrow{k_1} NpO_2^+ + {}^\bullet K \quad (4)$$

$${}^\bullet K \rightarrow \text{products} \quad (5)$$

The rate equation derived from this mechanism is

$$\text{rate} = k_1\beta_1 \frac{[\text{Np(VI)}][HK]_T}{1 + K_a[H^+] + \beta_1[HK]} \quad (6)$$

where k_1 is the rate constant for the rate-limiting step, β_1 is the stability constant for formation of NpO_2K^+, and K_a is the association constant for kojic acid. From $\log K_a = 7.67$ and $\log \beta_1 = 7.1$ (the value for formation of $[UO_2K^+]$[25,26]) the rate equation, for our conditions, can be reduced to

$$\text{rate} = \frac{k_1\beta_1}{K_a} \frac{[\text{Np(VI)}][HK]_T}{[H^+]} \quad (7)$$

From eq 1 and 7, we derive the relationship $k = k_1\beta_1/K_a$, which results in a value of $k_1 = 6.06 \pm 0.30$ s^{-1} at 25 °C and $\mu = 1.0$ M (NaCl).

Acknowledgment. This research was supported by a contract from the USDOE Office of Basic Energy Sciences, Division of Chemical Sciences.

Registry No. Np, 7439-99-8; kojic acid, 501-30-4.

(14) Woods, M.; Hoenich, C. L.; Sullivan, J. C. *J. Inorg. Nucl. Chem.* **1978**, *40*, 1907.
(15) Benson, D. *Mechanisms of Oxidation by Metal Ions*; Elsevier: New York, 1976; Chapter 2.
(16) Wells, C. F.; Kuritsyn, L. V. *J. Chem. Soc. A* **1970**, 1372.
(17) Wells, C. F.; Kuritsyn, L. V. *J. Chem. Soc. A* **1970**, 676.
(18) Davies, G.; Kustin, K. *Trans. Faraday Soc.* **1969**, *65*, 1630.
(19) Baxendale, J. H.; Hardy, H. R.; Sutcliffe, L. H. *Trans. Faraday Soc.* **1951**, *47*, 963.
(20) Wells, C. F.; Kuritsyn, L. V. *J. Chem. Soc. A* **1969**, 2930.
(21) Wells, C. F.; Kuritsyn, L. V. *J. Chem. Soc. A* **1969**, 2575.
(22) Mentasti, E.; Pelizzetti, E. *J. Chem. Soc., Dalton Trans.* **1973**, 2605.
(23) Mentasti, E.; Pelizzetti, E.; Saini, G. *J. Chem. Soc., Dalton Trans.* **1973**, 2609.
(24) Dixon, W. T.; Maghimi, M.; Murphy, D. *J. Chem. Soc., Perkin Trans. 2* **1975**, 101.
(25) Bartusek, M.; Sommer, L. *J. Inorg. Nucl. Chem.* **1965**, *27*, 2397.
(26) Martell, A. E.; Smith, R. M. *Critical Stability Constants*; Plenum: New York, 1977; Vol. 3.

Contribution from the Department of Chemistry, Purdue University, West Lafayette, Indiana 47907

Non-Metal Redox Kinetics: Oxidation of Iodide by Hypochlorous Acid and by Nitrogen Trichloride Measured by the Pulsed-Accelerated-Flow Method

Julius C. Nagy, Krishan Kumar, and Dale W. Margerum*

Received February 19, 1988

The very rapid reaction between HOCl and I^- is general-acid- (HA-) assisted. The proposed mechanism is

$$HOCl + I^- \underset{k_{-1}}{\overset{k_1}{\rightleftharpoons}} HOClI^-$$

$$HOClI^- \xrightarrow{k_0} HO^- + ICl$$

$$HOClI^- + HA \xrightarrow{k_{HA}} H_2O + ICl + A^-$$

$$ICl + 2I^- \xrightarrow{\text{fast}} I_3^- + Cl^-$$

where a stability constant ($k_1/k_{-1} = 220$ M^{-1}) is determined for the $HOClI^-$ intermediate from kinetic data and the limiting rate constant at high $[H^+]$ is $k_1 = 4.3 \times 10^8$ M^{-1} s^{-1}. Values for third-order rate constants (with the general form $k_1k_{HA}/(k_0 + k_{-1})$ (M^{-2} s^{-1}) at 25.0 °C, $\mu = 0.1$) are evaluated for H_3O^+ (3.5×10^{11}), CH_3COOH (3.2×10^{10}), and $H_2PO_4^-$ (2.6×10^{10}) and give a Brønsted α value of 0.11, which indicates a small degree of proton transfer in the transition state. For the H_2O path, $k_0k_1/(k_0 + k_{-1}) = 1.4 \times 10^8$ M^{-1} s^{-1}. The reaction between trichloramine and iodide exhibits saturation kinetics due to the formation of NCl_3I^- ($K_1 = 6 \times 10^3$ M^{-1}), which undergoes first-order decomposition ($k_2 = 1.5 \times 10^4$ s^{-1} at 25.0 °C and $\mu = 0.1$) to $HNCl_2$ and ICl. Acids do not affect the rate of NCl_3I^- decomposition. For these two studies first-order rate constants fall in the range of 10 000–142 000 s^{-1} and are measured by pulsed-accelerated-flow spectroscopy.

Introduction

Stopped-flow studies showed[1] that the reaction between OCl^- and I^- is general-acid-assisted with a Brønsted α value of 0.75. The third-order rate constant for $H_3O^+ + OCl^- + I^-$ is so large (4.4×10^{15} M^{-2} s^{-1}) that it is necessary to assume HOCl forms first (which is not the case for other acids) and that its reaction with I^- has a second-order rate constant of 1.4×10^8 M^{-1} s^{-1}. In the present study we examine the direct reaction between HOCl and I^- by use of pulsed-accelerated-flow (PAF) methods[2,3] and

(1) Kumar, K.; Day, R. A.; Margerum, D. W. *Inorg. Chem.* **1986**, *25*, 4344–4350.
(2) Jacobs, S. A.; Nemeth, M. T.; Kramer, G. W.; Ridley, T. Y.; Margerum, D. W. *Anal. Chem.* **1984**, *56*, 1058–1065.
(3) Nemeth, M. T.; Fogelman, K. D.; Ridley, T. Y.; Margerum, D. W. *Anal. Chem.* **1987**, *59*, 283–291.

0020-1669/88/1327-2773$01.50/0

confirm the value of the second-order rate constant. We find that the reaction is also general-acid-assisted but has a much smaller α value (0.11), as expected, because HOCl is a very weak base. Analogous reactions are known for Cl_2 formation (eq 1), which

$$H^+ + HOCl + Cl^- \rightleftarrows H_2O + Cl_2 \quad (1)$$

was studied by relaxation techniques,[4] and for BrCl formation (eq 2), which was studied by stopped-flow methods.[5] The re-

$$AH + HOCl + Br^- \rightarrow A^- + H_2O + BrCl \quad (2)$$

actions of interest in this work (eq 3) are extremely rapid and are

$$AH + HOCl + I^- \rightarrow A^- + H_2O + ICl \quad (3)$$

irreversible. Although they cannot be studied by stopped-flow or by relaxation techniques, they can be observed by the PAF method.

Two lines of kinetic evidence indicate that an $HOClI^-$ intermediate species is present in these reactions. As the I^- concentration increases at low acidities, there is a small, but noticeable, deviation from the initial first-order dependence in $[I^-]$. Secondly, as $[H^+]$ is increased above 10^{-3} M, a kinetic saturation effect is observed.

The rates of iodide oxidation by NH_2Cl and $NHCl_2$ also are general-acid-assisted,[1] and a general mechanism (eq 4) can be written, where the acid form of a buffer participates in the rate-determining step. In the transition state (**1**) a proton is

$$AH + ZCl + I^- \rightarrow A^- + HZ + ICl \quad (4)$$

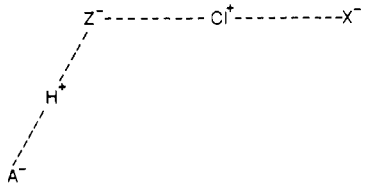

1

donated to the oxygen or nitrogen atom in the chlorine species (ZCl) as a bond forms between Cl and I^- and the Z–Cl bond is broken. The net result is a Cl^+ transfer to I^-. The rates decrease with the basicity of the chlorine species ($OCl^- \gg NH_2Cl \gg NHCl_2$). However, this trend reverses for HOCl and NCl_3, which both react very rapidly with I^- despite their extremely low basicity. The NCl_3 reaction with I^- is complete within the dead time of stopped-flow measurements, and all that is observed is the subsequent much slower reaction of $NHCl_2$ and I^-. Therefore, the NCl_3 reactions also are studied by the PAF method.

One of the initial reaction products is ICl, which reacts with excess I^- (1.1×10^9 M^{-1} s^{-1}, obtained by PAF methods)[6] to give I_2 (eq 5), and I_2 reacts with I^- (6.2×10^9 M^{-1} s^{-1}, obtained by relaxation methods)[7] to give I_3^- (eq 6). The appearance of I_3^-

$$ICl + I^- \rightarrow I_2 + Cl^- \quad (5)$$

$$I_2 + I^- \rightleftarrows I_3^- \qquad K = 740\ M^{-1} \quad (6)$$

is a convenient way to follow the progress of these reactions due to its large molar absorptivity ($\epsilon = 26\,400$ M^{-1} cm^{-1}) at 353 nm.[8]

Studies that involve NCl_3 are difficult for several reasons. The pure compound undergoes spontaneous explosions,[9,10] and its isolation is not recommended. Dilute acidic solutions of NCl_3 are relatively stable but invariably contain small amounts of HOCl. The vapor pressure of NCl_3 is 150 Torr at room temperature,[11] so it is very volatile and easily lost from aqueous solution. Although its reaction with iodide is used for analytical methods, the yield of I_2 from NCl_3 is only about 80% of the theoretical amount.[1] Despite these problems we are able to measure the very fast rate of I_3^- produced when NCl_3 reacts with I^-. The reaction is nearly independent of the iodide concentration due to the formation of a complex (NCl_3I^-) with a large association constant (6×10^3 M^{-1}). The reaction is not assisted by buffer acids and does not have a $[H^+]$ dependence.

Experimental Section

Solutions of HOCl were prepared by dilution of 10% NaOCl solution (Mallinckrodt) into buffered or $HClO_4$ media, which was first filtered and degassed for use with the PAF spectrometer. Some experiments were performed with dilutions of a NaOCl solution prepared by the passage of Cl_2 through concentrated NaOH. These solutions were used only for 1–2 weeks to minimize the degree of contamination from OCl^- decomposition products.[12] The absorbance at 235 nm ($\epsilon = 100$ M^{-1} cm^{-1})[13] was used to determine the concentration of HOCl. The $-\log [H^+]$ values of buffered solutions were adjusted prior to the addition of NaOCl, and these values were redetermined after the kinetic measurements.

Solutions of NCl_3 were prepared from a mixture of 3 equiv of HOCl and 1 equiv of NH_3, with both solutions initially below pH 3.5. The NH_3 stock solution was standardized by titration with $HClO_4$ with bromocresol green as the indicator. The HOCl and NH_3 solutions were mixed through a twin-jet mixer, and the resulting NCl_3 solutions were kept overnight to allow all side reactions to go to completion. The concentration of NCl_3 was determined spectrophotometrically at 336 nm ($\epsilon = 195$ M^{-1} cm^{-1}).[14] Immediately after standardization the NCl_3 solution was divided into small containers with no headspace. These containers were stoppered and covered to exclude light. Only one aliquot was drawn from each of these containers in an attempt to minimize the loss of NCl_3 due to volatility. All necessary $-\log [H^+]$ adjustments, filtration, and degassing were performed prior to the addition of NCl_3 to the reaction media.

Buffer solutions were prepared from NaH_2PO_4 and NaOH and from CH_3COONa and dilute $HClO_4$. Solutions of NaI were flushed with argon to remove oxygen. The NaI was standardized[15] by oxidation of iodide to iodate with bromine (excess bromine was removed by boiling), followed by addition of excess NaI and HCl, and titration with a standardized solution of $Na_2S_2O_3$. All solutions were prepared with distilled, deionized water. The ionic strength was controlled with recrystallized $NaClO_4$. Perchloric acid was standardized with a NaOH solution that in turn was standardized with potassium hydrogen phthalate.

A Sargent-Welch No. S-30072-15 combination electrode connected to an Orion Research Model 601 Ionanalyzer was used to measure pH. These pH values were corrected to $-\log [H^+]$ values with electrode parameters that were obtained via a strong-acid–strong-base titration, with subsequent analysis of the titration data by the method of Gran,[16] followed by a linear regression of measured pH and calculated $-\log [H^+]$ values.

UV–vis spectral data were obtained with a Perkin-Elmer Model 320 spectrophotometer. Data were collected at a temperature of 25.0 (±0.1) °C. A spectrum of a blank of the appropriate composition was stored in memory and automatically subtracted from all scans.

A Durrum stopped-flow spectrophotometer interfaced[17] to a Hewlett-Packard 2100S minicomputer was used to determine the amount of HOCl in NCl_3 solutions by reaction with bromide. The formation of Br_2/Br_3^- was monitored at 360 nm ($\epsilon_{Br_2} = 175$ M^{-1} cm^{-1}, $\epsilon_{Br_3} = 600$ M^{-1} cm^{-1}, with a formation constant of 17 M^{-1}).[5] The absorbances of the NaBr and NCl_3/HOCl solutions were then determined. The traces for the reaction of Br^- with a mixture of NCl_3 and HOCl show that two reactions take place. The first, between HOCl and Br^-, is observed as an absorbance jump. A study of the reaction of HOCl and Br^- reports[5] an expression for k_{obsd} in buffered solutions (eq 7), where k'' is $1.55 \times$

$$k_{obsd} = (k'' + k_H''[H^+] + k_{HA}''[HA])[Br^-] \quad (7)$$

(4) Eigen, M.; Kustin, K. *J. Am. Chem. Soc.* **1962**, *84*, 1355–1361.
(5) Kumar, K.; Margerum, D. W. *Inorg. Chem.* **1987**, *26*, 2706–2711.
(6) Margerum, D. W.; Dickson, P. N.; Nagy, J. C.; Kumar, K.; Bowers, C. P.; Fogelman, K. D. *Inorg. Chem.* **1986**, *25*, 4900–4904.
(7) Turner, D. H.; Flynn, G. W.; Sutin, N.; Beitz, J. V. *J. Am. Chem. Soc.* **1972**, *94*, 1554–1559.
(8) Awtrey, A. D.; Connick, R. E. *J. Am. Chem. Soc.* **1951**, *73*, 1341–1348.
(9) Kumar, K.; Shinness, R. W.; Margerum, D. W. *Inorg. Chem.* **1987**, *26*, 3430–3434.
(10) Work of P. L. Dulong, reported by: Thenard, L. J.; Berthollet, C. L. *Ann. Chim. (Paris)* **1813**, *86*, 37–43.
(11) *The Merck Index*, 9th ed.; Windholz, M., Ed.; Merck: Rahway, NJ, 1976; p 858.
(12) Chapin, R. M. *J. Am. Chem. Soc.* **1934**, *56*, 2211–2215.
(13) Gray, E. T., Jr. Ph.D. Thesis, Purdue University, West Lafayette, IN, 1977.
(14) Hand, V. C. Ph.D. Thesis, Purdue University, West Lafayette, IN, 1982.
(15) Kolthoff, I. M.; Sandall, E. B.; Meehan, E. J.; Bruckenstein, S. *Quantitative Chemical Analysis*, 4th ed.; Macmillan: London, 1969; p 852.
(16) Rossotti, F. J.; Rossotti, H. *J. Chem. Educ.* **1965**, *42*, 375–378.
(17) Willis, B. G.; Bittikofer, J. A.; Pardue, H. L.; Margerum, D. W. *Anal. Chem.* **1970**, *42*, 1340–1349.

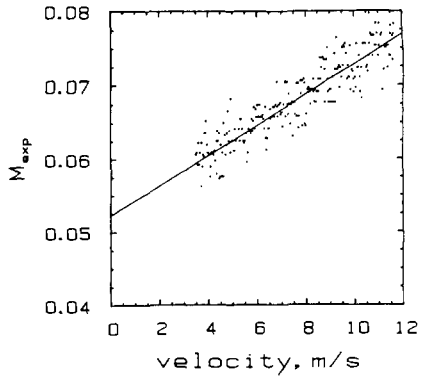

Figure 1. Experimental data for the reaction of HOCl and I^- obtained by the pulsed-accelerated-flow method. The solid line is a least-squares fit of eq 12. Conditions: [HOCl] = 1.0×10^{-5} M; [I^-] = 0.245×10^{-3} M; [H^+] = 1.70×10^{-3} M; μ = 0.1; 25.0 °C. The rate constant for this data set is 49 (±2) × 10^3 s^{-1}.

10^3 M^{-1} s^{-1}, k_H'' is 1.32×10^6 M^{-2} s^{-1}, and k_{HOAc}'' (for CH_3COOH) is 2.09×10^4 M^{-2} s^{-1}. The [H^+], $[OAc]_T$, and [Br^-] values were adjusted to make the HOCl + Br^- reaction complete within the dead time of the stopped-flow instrument. The absorbance jump is used to calculate $[HOCl]_0$ in the NCl_3 solution. The second reaction, between NCl_3 and Br^-, is measurable on the stopped-flow instrument. At $[OAc]_T$ = 0.1 M, −log [H^+] = 4.68, [Br^-] = 0.2 M, and μ = 0.5, the pseudo-first-order rate constant for NCl_3 + Br^- was found to be 1.93 (5) s^{-1}. As is the case with the iodide reaction[1] with NCl_3, the stoichiometry of the reaction is not known.

Pulsed-Accelerated-Flow Method. A pulsed-accelerated-flow spectrometer, Model IV,[18] was used to obtain kinetic data for the reactions of iodide with HOCl and with NCl_3. This instrument has a wavelength range of 200–850 nm. Improvements in the optics of the instrument lead to much higher throughput as compared to that of earlier models.[2,3] The PAF spectrometer employs integrating observation[19,20] during continuous-flow mixing of short duration (a 0.4-s pulse). The purpose of the pulsed flow is to conserve reagents.[2,3] The reactants are observed along the direction of flow from their point of mixing to their exit from the observation tube (1.025 cm). A twin-path mixing/observation cell made from poly(vinyl chloride) was used.[3] In this study, the flow was decelerated during the pulse to give a linear velocity ramp,[21] and 250 measurements of the transmittance were taken as the flow velocity in the observation tube changed from 12.5 to 3.0 m s^{-1}. The velocity variation permits the chemical process to be resolved from the mixing process.[2,3] The method of observation, the efficient mixing, and the variation of flow velocity permit accurate measurement of first-order rate constants as large as 180000 s^{-1}.[3,18] This is a factor of 10^3 larger than can be measured by typical stopped-flow methods. Solution reservoirs, drive syringes, and the mixing/observation cell were thermostated at 25.0 (±0.2) °C with a circulating water bath. Reactant solutions were drawn directly from the reservoirs into the drive syringes through Teflon tubing.

The fundamental relationship used in the analysis of first-order PAF data is given in eq 8, where M_{exptl} is the defined absorbance ratio, A_v is the absorbance of the reaction mixture at a given instantaneous velocity, A_∞ is the absorbance at infinite time, A_0 is the absorbance at time zero, k_{app} is the apparent rate constant (s^{-1}), b is the reaction path length (=0.010 25 m), v is the solution velocity in the observation tube (m s^{-1}), and Y is a parameter that is iterated to fit the equation.[19,20] All ab-

$$M_{exptl} = \frac{A_v - A_\infty}{A_0 - A_\infty} = \frac{1 - e^{-Y}}{Y} \qquad Y = \frac{bk_{app}}{v} \tag{8}$$

sorbances are measured in the PAF spectrometer. The apparent rate constant, k_{app}, is related to the reaction rate constant, k_r (s^{-1}), and a mixing rate constant, k_{mix} (s^{-1}), by eq 9.[2,3] The mixing rate constant,

$$\frac{1}{k_{app}} = \frac{1}{k_{mix}} + \frac{1}{k_r} \tag{9}$$

k_{mix}, depends on the velocity (eq 10), where k_m is a mixing constant.

$$k_{mix} = k_m v \tag{10}$$

(18) Fogelman, K. D.; Bowers, C. P.; Nagy, J. C.; Ridley, T. Y.; Wang, Y. L.; Margerum, D. W., to be submitted for publication.
(19) Gerischer, H.; Heim, W. *Z. Phys. Chem. (Munich)* **1965**, *46*, 345–352.
(20) Gerischer, H.; Heim, W. *Ber. Bunsen-Ges. Phys. Chem.* **1967**, *71*, 1040–1046.
(21) Nagy, J. C. Ph.D. Thesis, Purdue University, West Lafayette, IN, 1988.

Table I. Iodide Dependence of the Pseudo-First-Order Rate Constants for the Reaction of HOCl and Excess I^- [a]

10^3[I^-], M	10^5[HOCl], M	$10^{-3}k_r$, s^{-1}	10^3[I^-], M	10^5[HOCl], M	$10^{-3}k_r$, s^{-1}
0.196	0.81	16.7 (7)	0.491	1.63	42 (1)
0.294	0.81	25.0 (3)	0.736	1.63	58.1 (3)
0.392	1.63	32.1 (8)	0.981	3.25	73 (1)

[a] $[PO_4]_T = 1.0 \times 10^{-3}$ M; −log [H^+] = 7.30.

Typically, k_m is greater than 1700 m^{-1} and v is 3.0–12.5 m s^{-1}. For first-order rate constants greater than 4000 s^{-1}, $\exp(-Y) \ll 1$ in eq 8 and the model simplifies to eq 11. Substitution of eq 9 and 10 into eq 11

$$M_{exptl} = \frac{A_v - A_\infty}{A_0 - A_\infty} = \frac{1}{Y} = \frac{v}{bk_{app}} \tag{11}$$

$$M_{exptl} = \frac{A_v - A_\infty}{A_0 - A_\infty} = \frac{1}{bk_m} + \frac{v}{bk_r} \tag{12}$$

yields eq 12, where M_{exptl} is a linear function of velocity for fast reactions. Plots of M_{exptl} vs v (Figure 1) have slopes of $1/(bk_r)$ and intercepts of $1/(bk_m)$ for first-order reactions. Experimental data for the kinetics of I_3^- formation (observed at 353 nm) from solutions of HOCl and I^-, and from NCl_3 and I^-, obey the model of eq 12 over the entire range of rate constants studied. The pseudo-first-order rate constants (k_r, s^{-1}) reported in this work are obtained from linear regressions of M_{exptl} vs v plots. All kinetic data obtained on the PAF spectrometer were collected under the following conditions: μ = 0.1 (with $NaClO_4$), 25.0 °C, and λ = 353 nm. The k_r values reported in the tables are averages of at least three trials. The values in parentheses denote one standard deviation in the last digit.

Results and Discussion

Series Reactions and PAF Measurements. The large molar absorptivity of I_3^- not only makes it a useful indicator to study the rate of reaction between HOCl and I^- but also makes it difficult to observe other species directly. As the reaction is carried out in a large excess of I^-, triiodide is formed at the end of a series of reactions (eq 13a) that can be designated by the labels in eq 13b. The integrating observation used in the PAF measurements

$$HOCl + I^- \xrightarrow{H^+} ICl \xrightarrow{I^-} I_2 \overset{I^-}{\rightleftharpoons} I_3^- \tag{13a}$$

$$A \xrightarrow{k_{AB}} B \xrightarrow{k_{BC}} C \underset{k_{DC}}{\overset{k_{CD}}{\rightleftharpoons}} D \tag{13b}$$

responds to the absorbance changes for all the reactions that take place from initial mixing until the time of exit from the observation tube. If the solutions were brought together with perfect mixing (i.e. the reactant mixture was instantaneously homogeneous as it entered the observation tube), the ratio of rate constants[1,6] for k_{BC}/k_{AB} would be 1.1×10^9 M^{-1} s^{-1}/1.4×10^8 M^{-1} s^{-1} = 7.9 (provided the A to B reaction is not acid catalyzed). This would cause a small buildup of the intermediate ICl species in accord with eq 14,[22] such that $[ICl]_{max}$ would reach 8.6% of $[HOCl]_0$.

$$[ICl]_{max}/[HOCl]_0 = \left(\frac{k_{BC}}{k_{AB}}\right)^{k_{BC}/(k_{AB}-k_{BC})} \tag{14}$$

The buildup and decay of ICl would cause the formation of I_3^- to lag behind the reaction of HOCl and I^-. However, the fact that mixing is not instantaneous is an advantage in these measurements. The rate of formation of ICl is influenced greatly by the mixing rate, and the apparent rate constant (k_{app}) for its formation is much smaller than the product (1.4×10^8)[I^-] (=k_r), in accord with eq 9. On the other hand, the solution is already mixed after ICl forms, so that the k_{BC} rate constant (=(1.1×10^9)[I^-] s^{-1}) for the formation of I_2 and k_{CD} for the formation of I_3^- are not seriously affected by the mixing process. The C ⇄ D step behaves as a reversible first-order process, where k_{obsd} = $k_{CD} + k_{DC}$ (k_{CD} = 6.2×10^9 M^{-1} s^{-1} and k_{DC} = 8.5×10^6 s^{-1}),[7]

(22) Espenson, J. H. *Chemical Kinetics and Reaction Mechanisms*; McGraw-Hill: New York, 1981; p 66.

so it is a relatively fast process. The final ratio of I_3^-/I_2 varies from 0.15 to 0.73 as the I^- concentration increases. This permits the observed formation of I_3^- to be used as an indicator for the A to B step.

For example, consider the conditions used for the lowest I^- concentration (0.196×10^{-3} M) in Table I at $-\log [H^+] = 7.30$. The velocity range is 3–12 m s^{-1} and $k_m = 2000$ m^{-1}, so that $k_{mix} = 6000$–$24\,000$ s^{-1} (eq 10). The predicted value for k_r (eq 15)

$$k_r = (1.4 \times 10^8\ M^{-1}\ s^{-1})[I^-]f_{HOCl} \qquad f_{HOCl} = [H^+]/([H^+] + K_a) \tag{15}$$

is 15 920 s^{-1}. In eq 15, f_{HOCL} is the fraction of $[HOCl]_T$ in the form of HOCl ($f_{HOCl} = 0.58$), because the pK_a of HOCl is 7.44.[13] From eq 9, at $v = 3$ m s^{-1}, $k_{app(3)} = 4360$ s^{-1}, while at $v = 12$ m s^{-1}, $k_{app(12)} = 9570$ s^{-1}. Since k_{BC} is unaffected by mixing, the ratio k_{BC}/k_{AB} changes from 49.4 to 22.5 during the velocity change in the PAF measurement. This predicts that $[ICl]_{max}$ should reach only 1.8% of $[HOCl]_T$ at $v = 3$ m s^{-1} and 3.7% of $[HOCl]_T$ at $v = 12$ m s^{-1}. The deviation that this causes in the change of the integrated absorbance with velocity is smaller than the experimental error of the measurements. The experimental value of k_r under these conditions is $16\,700 \pm 700$ s^{-1}. This is very close to the predicted value of 15 920 s^{-1}, and as we shall see the predicted value should be slightly larger due to the presence of 2.4×10^{-4} M $H_2PO_4^-$, which assists the reaction.

As the I^- concentration increases (from 0.2 to 1.0 mM in Table I), the k_{BC} and k_{CD} rate constants increase 5-fold, but the k_{AB} rate constants change much less because the k_{mix} values dominate k_{app} and are unchanged. Therefore, the buildup of ICl is much smaller and I_3^- formation is a suitable indicator for the reactions of HOCl with the full range of I^- concentrations under the conditions in Table I.

Iodide Dependence of the HOCl Reaction. The reaction of a mixture of OCl^- and HOCl ($-\log [H^+] = 7.30$ and $[PO_4]_T = 1.0 \times 10^{-3}$ M) with excess I^- gives excellent M_{exptl} vs v plots, and k_r values vary from 16 700 to 73 000 s^{-1} as the I^- concentration increases (Table I). The k_r values are the averages of at least three runs, and the standard deviations range from 1.4 to 4.1%.

The rate of the proton-transfer reaction (eq 16) can be calculated,[23] on the basis of a positive ΔpK_a value (7.44 – 6.80), to be approximately 10^9 M^{-1} s^{-1} at $\mu = 0.1$ and 25.0 °C. Even the

$$H_2PO_4^- + OCl^- \rightleftarrows HPO_4^{2-} + HOCl \tag{16}$$

lowest concentration of $H_2PO_4^-$ (2.4×10^{-4} M) is sufficient to ensure that the pseudo-first-order proton-transfer rate constant (2.4×10^5 s^{-1}) is much larger than the measured k_r values and that the reactions are not limited by the proton transfer in eq 16.

The reaction of HOCl and I^- is first order in $[I^-]$ at the lower iodide concentrations used, but some deviation from linear behavior is seen at $[I^-] > 0.4 \times 10^{-3}$ M (Figure 2). This behavior indicates saturation kinetics, or the existence of a rapid preequilibrium step prior to the rate-determining step. We propose a mechanism for this system (eq 17 and 18) that goes through an $HOCII^-$ species,

$$HOCl + I^- \underset{k_{-1}}{\overset{k_1}{\rightleftharpoons}} HOCII^- \tag{17}$$

$$HOCII^- \xrightarrow{k_0} OH^- + ICl \tag{18}$$

which decomposes (k_0) to form OH^- and ICl. The ICl formed reacts rapidly with excess I^- to form I_3^- (eq 5 and 6). The rate law is given in eq 19, where it is initially assumed that a preequilibrium exists for $HOCII^-$ with a stability constant of K_1'. As given in eq 15, we need to account for the fraction of $[OCl^-]_T$ that exists as HOCl at $-\log [H^+] = 7.30$, and this combined with eq 19 gives the relationship between k_r and $[I^-]$ (eq 20). Rearrangement of eq 20 yields a linear form (eq 21) that can be used to resolve values for K_1' and k_0. The values determined are $K_1' = (1.5 \pm 0.5) \times 10^2$ M^{-1} and $k_0 = (1.0 \pm 0.3) \times 10^6$ s^{-1}, and the solid line in Figure 2 is calculated from these values and eq 20.

$$\text{rate} = \frac{K_1'k_0[I^-]}{1 + K_1'[I^-]}[HOCl] \tag{19}$$

$$k_r = \left(\frac{K_1'k_0[I^-]}{1 + K_1'[I^-]}\right)\frac{[H^+]}{[H^+] + K_a^{HOCl}} \tag{20}$$

$$\frac{[H^+]}{([H^+] + K_a^{HOCl})k_r} = \frac{1}{K_1'k_0}\frac{1}{[I^-]} + \frac{1}{k_0} \tag{21}$$

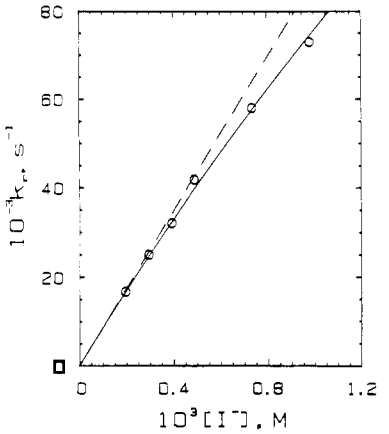

Figure 2. Pseudo-first-order rate constants vs $[I^-]$, the excess reagent, for the reaction between HOCl and I^-. The solid line utilizes the full expression in eq 20. The dashed line represents the case where $[HOCII^-]$ is negligible and saturation kinetics are not observed.

Hydrogen Ion Dependence of the HOCl and I^- Reaction. The kinetics of the reaction were studied with variation of $[H^+]$ from 0.454×10^{-3} to 3.97×10^{-3} M. The HOCl and I^- solutions were adjusted to the same $[H^+]$ before mixing. The iodide concentrations used were in the range where a first-order $[I^-]$ dependence was observed at $-\log [H^+] = 7.30$. The iodide concentrations were selected to be low enough to avoid appreciable formation of $HOCII^-$ and to be high enough to permit I_3^- formation to serve as a suitable probe of the kinetics without appreciable buildup of the ICl intermediate. As the $[H^+]$ increased, the reaction rate increased and it was necessary to increase $[I^-]$ from 0.245×10^{-3} to 0.390×10^{-3} M to meet these criteria. Unfortunately, the I^- concentration cannot be increased further without making the k_r values too large to be measured by the PAF method.

Division of the pseudo-first-order rate constants in Table II by $[I^-]$ gives second-order rate constants that initially increase with $[H^+]$ and then appear to level off (Figure 3). This behavior is consistent with saturation kinetics in $[H^+]$, and the mechanism must have a proton-assisted path. The results suggest a mechanism with a H^+-assisted breakup of $HOCII^-$ (eq 22) in addition to the steps in eq 17 and 18. The rate law becomes eq 23. Rearrangement of eq 23 yields eq 24, which can be used to determine a value for k_1 (4.3 (± 0.3) $\times 10^8$ M^{-1} s^{-1}) and k_H/k_0 (2.5 (± 0.5) $\times 10^3$ M^{-1}). The fit of the model to the data was performed with

$$H^+ + HOCII^- \xrightarrow{k_H} H_2O + ICl \tag{22}$$

$$\text{rate} = \frac{k_1(k_0 + k_H[H^+])[I^-][HOCl]}{k_{-1} + k_0 + k_H[H^+]} \tag{23}$$

$$\frac{\text{rate}}{[HOCl]_T[I^-]} = \frac{k_r}{[I^-]} = \frac{1 + \frac{k_H}{k_0}[H^+]}{\frac{k_{-1} + k_0}{k_1k_0} + \frac{k_H[H^+]}{k_0k_1}} \tag{24}$$

(23) Eigen, M. *Angew. Chem., Int. Ed. Engl.* **1964**, *3*, 1–72.

Table II. Acid Dependence of the Reaction between HOCl and I^- [a]

$10^3[I^-]$, M	$10^3[H^+]$, M	$10^{-3}k_r$, s^{-1}	$10^3[I^-]$, M	$10^3[H^+]$, M	$10^{-3}k_r$, s^{-1}
0.245	0.454	50 (2)	0.390	1.70	122 (4)
0.368	0.907	98 (2)	0.390	2.27	120 (8)
0.390	1.13	115 (5)	0.390	3.97	142 (4)

[a] $[HOCl] = 1.0 \times 10^{-5}$ M.

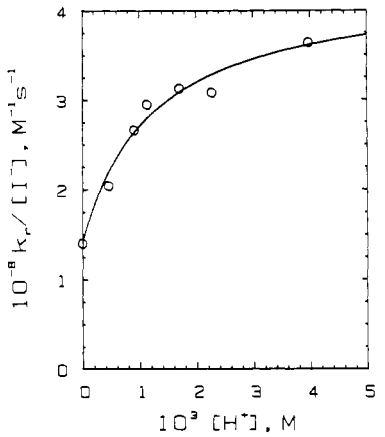

Figure 3. Plot of the second-order rate constants vs $[H^+]$ for the reaction of HOCl and I^- obtained in $HClO_4$ medium. The solid curve is calculated from the rate constants in Table IV for the model given in eq 24.

a simplex optimization procedure.[24,25] At $[H^+] = \infty$, eq 24 reduces to eq 25, which means that k_1 is the limiting rate constant. As

$$k_r/[I^-] = k_1 \tag{25}$$

$[H^+]$ approaches zero, eq 24 reduces to eq 26, which is the expression for the value (1.4×10^8 M^{-1} s^{-1}) determined previously from the inverse $[OH^-]$ dependence in the reaction of OCl^- and I^-.[1] This value can be used along with the value of k_1 to determine the k_{-1}/k_0 ratio, which equals 2.1.

$$\frac{k_r}{[I^-]} = \frac{k_1k_0}{k_{-1} + k_0} = k_{HOCl} \tag{26}$$

The fact that k_{-1} is not much greater than k_0 means that the first step in this mechanism is not a rapid preequilibrium. The study in acidic solutions was carried out at a high enough H^+ concentration and with $[I^-]$ sufficiently low that a steady-state condition was reached, with negligible concentrations of $HOClI^-$ present. However, the iodide-dependence study was carried out under conditions where an appreciable amount of $HOClI^-$ was formed, and K_1' and k_0 must be corrected to reflect this fact. The apparent equilibrium constant, K_1', is more accurately represented by eq 27. Rearrangement yields eq 28, and the corrected

$$K_1' = \frac{k_1}{k_{-1} + k_0} \tag{27}$$

$$\frac{k_1}{k_{-1}} = K_1 = 1.5K_1' \tag{28}$$

equilibrium constant, K_1, has a value of $(2.2 \pm 0.7) \times 10^2$ M^{-1}. Values for k_{-1} (1.9×10^6 s^{-1}), k_0 (9.0×10^5 s^{-1}), and k_H (2.3×10^9 M^{-1} s^{-1}) are calculated through the use of K_1, k_1, and the values for k_{-1}/k_0 and k_H/k_0.

General-Acid-Assisted Reactions in Buffered Solutions. The existence of a H^+ path, along with the general-acid-assisted mechanism for the oxidation of iodide by OCl^-, NH_2Cl, and $NHCl_2$,[1] suggest that a general-acid-assisted path may also be active for HOCl + I^-. Therefore, $[PO_4]_T$, $[OAc]_T$, and $-\log [H^+]$ values were varied, and the observed pseudo-first-order rate constants (Table III) show that general-acid-assisted reactions do occur.

(24) Caceci, M. S.; Catheris, W. P. *Byte* **1984**, *9*, 340–362.
(25) Yarboro, L. A.; Deming, S. N. *Anal. Chim. Acta* **1974**, *73*, 391–398.

Table III. Kinetic Data for the Reaction of HOCl and I^-: [HA] Dependence[a]

$10^3[HA]_T$, M	$-\log [H^+]$	$10^{-3}k_r$, s^{-1}	$10^3[HA]_T$, M	$-\log [H^+]$	$10^{-3}k_r$, s^{-1}
		Phosphate Buffer[b]			
1.0	7.31	21 (1)	2.0	6.07	39 (1)
2.0	7.31	20.1 (9)	3.0	6.07	38 (3)
3.0	7.31	22.0 (7)	4.0	6.07	47 (3)
5.0	7.30	23.4 (2)	5.0	6.08	48.1 (5)
10.0	7.30	25.1 (6)	1.0	5.96	34.6 (7)
1.0	6.48	32 (2)	2.0	5.85	35.6 (4)
2.0	6.48	36 (1)	3.0	5.81	40 (1)
3.0	6.46	39.5 (9)	4.0	5.82	45 (2)
5.0	6.46	47.8 (8)	5.0	5.83	46 (4)
1.0	6.06	34 (2)			
		Acetate Buffer[c]			
1.0	4.24	33 (3)	3.0	4.59	37 (2)
2.0	4.23	33 (1)	1.0	4.84	27 (2)
3.0	4.21	36 (2)	2.0	4.82	27.6 (6)
1.0	4.58	31.8 (6)	3.0	4.81	32 (3)
2.0	4.58	32 (2)	5.0	4.81	33 (1)

[a] $[HOCl] = 1.0 \times 10^{-5}$ M. [b] $[I^-] = 0.245 \times 10^{-3}$ M. [c] $[I^-] = 0.242 \times 10^{-3}$ M.

Table IV. Resolved Rate Constants for the HOCl + I^- Reaction[a]

param	resolved value
K_1'	$(1.5 \pm 0.5) \times 10^2$ M^{-1}
K_1	$(2.2 \pm 0.7) \times 10^2$ M^{-1}
k_1	$(4.3 \pm 0.3) \times 10^8$ M^{-1} s^{-1}
k_{-1}	$(1.9 \pm 0.7) \times 10^6$ s^{-1}
$k_{HOCl} = k_1k_0/(k_{-1} + k_0)$	1.4×10^8 M^{-1} s^{-1}
k_0	$(9 \pm 3) \times 10^5$ s^{-1}
$k_{H_3O}' = k_1k_H/(k_{-1} + k_0)$	3.5×10^{11} M^{-2} s^{-1}
k_H	$(2.3 \pm 0.5) \times 10^9$ M^{-1} s^{-1}
$k_{H_2PO_4}' = k_1k_{H_2PO_4}/(k_{-1} + k_0)$	2.6×10^{10} M^{-2} s^{-1}
$k_{H_2PO_4}$	$(1.7 \pm 0.6) \times 10^8$ M^{-1} s^{-1}
$k_{HOAc}' = k_1k_{HOAc}/(k_{-1} + k_0)$	3.2×10^{10} M^{-2} s^{-1}
k_{HOAc}	$(2.1 \pm 0.9) \times 10^8$ M^{-1} s^{-1}

[a] $\mu = 0.1$; 25.0 °C.

Addition of a general-acid-assisted path to the mechanism gives the full set of equations (eq 29–34) for the mechanism (resolved values for the rate constants are given in Table IV), with the rate law given in eq 35.

$$HOCl + I^- \underset{k_{-1}}{\overset{k_1}{\rightleftharpoons}} HOClI^- \tag{29}$$

$$HOClI^- \xrightarrow{k_0} OH^- + ICl \tag{30}$$

$$H^+ + HOClI^- \xrightarrow{k_H} H_2O + ICl \tag{31}$$

$$HA + HOClI^- \xrightarrow{k_{HA}} A^- + H_2O + ICl \tag{32}$$

$$ICl + I^- \xrightarrow{fast} I_2 + Cl^- \tag{33}$$

$$I_2 + I^- \underset{}{\overset{fast}{\rightleftharpoons}} I_3^- \tag{34}$$

$$\text{rate} = \frac{k_1(k_0 + k_H[H^+] + k_{HA}[HA])[I^-][HOCl]}{k_{-1} + k_0 + k_H[H^+] + k_{HA}[HA]} \tag{35}$$

The rate law can be simplified when the $k_H[H^+]$ term in the denominator is significantly less than $k_{-1} + k_0$, so that $k_H[H^+]$ can be dropped from the expression. In phosphate buffer, the lowest $-\log [H^+]$ value used was 5.81 and the product $k_H[H^+]$ equals 3.6×10^3 s^{-1}, while $k_{-1} + k_0$ equals 2.9×10^6 s^{-1}. Therefore, the $k_H[H^+]$ term can be dropped from the denominator and the numerator. The simplified rate law is rearranged into a form (eq 36) that is used to determine k_{HA}. A simplex optimization pro-

$$\frac{\text{rate}}{[HOCl]_T[I^-]} = \frac{k_r}{[I^-]f_{HOCl}} = \frac{k_1(k_0 + k_{HA}[HA])}{k_{-1} + k_0 + k_{HA}[HA]} \tag{36}$$

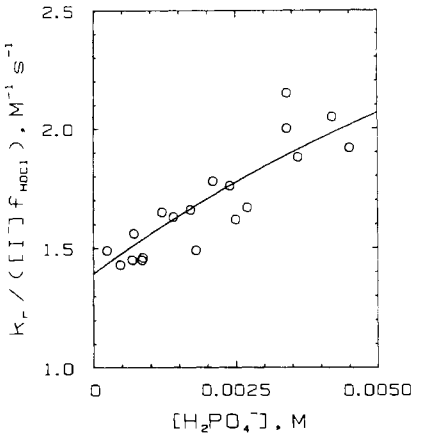

Figure 4. Plot of the second-order rate constants vs $[H_2PO_4^-]$ for the reaction of HOCl and I^- obtained in phosphate buffer ($f_{HOCl} = [H^+]/([H^+] + K_a^{HOCl})$). The solid curve is calculated from the rate constants in Table IV fit to eq 36.

cedure[24,25] was used to fit eq 36 to the kinetic data collected in phosphate buffer where both total phosphate, $[HA]_T$, and $-\log [H^+]$ were varied (Table III). A pK_a value of 6.80 was used for $H_2PO_4^-$, and the fit of eq 36 is shown in Figure 4, where $k_{H_2PO_4} = 1.7\ (\pm 0.6) \times 10^8\ M^{-1}\ s^{-1}$. There is a considerable amount of scatter in the data, and eq 36 fits only slightly better than a linear relationship between k_r and the $H_2PO_4^-$ concentration. The intercept when $[HA] = 0$ corresponds to k_{HOCl}(eq 26) $= 1.4 \times 10^8\ M^{-1}\ s^{-1}$.

In acetate buffer the maximum contribution of the $k_H[H^+]$ term is small (14% of the k_0 term in the numerator and 5% of the $k_{-1} + k_0$ term in the denominator of eq 35). Again the data are somewhat scattered and the intercept for $[HA] = 0$ is a little low, but the value obtained for k_{HOAc} is $2.1\ (\pm 0.9) \times 10^8\ M^{-1}\ s^{-1}$.

Brønsted Relationship for the Reaction of HOCl and I^- with HA. Determination of the Brønsted α value for this reaction allows comparisons to other general-acid-assisted reactions. The α value reflects the sensitivity of the rate to the strength of the general acid. Therefore, it describes the degree of proton transfer from the general acid to the substrate in the transition state (**1**).[26] In order to make this comparison, the transition state is considered to be the species where H^+ is transferred from HA to $HOClI^-$ as the O–Cl bond is broken and ICl is liberated. In the present case, third-order rate constants are obtained through the use of eq 37, where k_{HA}' is the third-order rate constant (Table IV) that

$$k_{HA}' = \frac{k_1}{k_{-1} + k_0} k_{HA} \tag{37}$$

$$HA + HOCl + I^- \xrightarrow{k_{HA}'} A^- + H_2O + ICl \tag{38}$$

describes the reaction in eq 38 (shown in **1**). The values are $k_{H_2PO_4}' = 2.6 \times 10^{10}\ M^{-2}\ s^{-1}$, $k_{HOAc}' = 3.2 \times 10^{10}\ M^{-2}\ s^{-1}$, and $k_{H_3O}' = 3.5 \times 10^{11}\ M^{-2}\ s^{-1}$. The magnitude of the value for the proton-assisted (H_3O^+) path is larger than is possible for a three-body reaction and dictates that two of the three molecules must form an association complex before the reaction can actually take place. It has already been assumed that $HOClI^-$ is the association complex that is formed. An alternative assumption that an appreciable amount of H_2OCl^+ exists in this pH range is not valid. The pK_a value for H_2OCl^+ is reported to be between -4 and -3.[27] There cannot be an appreciable concentration of H_2OCl^+ at any acidity in water.

The Brønsted relationship[28] is given by the expression in eq 39, where p is the number of equivalent acidic protons in HA, q is the number of equivalent basic sites in A^-, and G_A is a proportionality constant. A plot of $\log (k_{HA}'/p)$ vs $\log (K_a q/p)$ should

$$\frac{k_{HA}'}{p} = G_A \left(\frac{K_a q}{p} \right)^{\alpha} \tag{39}$$

give a line with a slope equivalent to the α value. The data used are in Table V, and the plot is shown in Figure 5, where the α value is determined to be 0.11 ± 0.01. The k_{H_2O} point was not used in the calculation of α since it obviously does not fit the trend shown in the other three points. It is not clear that H_2O actually acts as an acid in these reactions, and this may be the reason it does not fit the Brønsted relationship.

Table V. Summary of Constants for the Brønsted Relationship

HA	p	q	pK_a	k_{HA}',[a] $M^{-2}\ s^{-1}$	log (k_{HA}'/p)	log $(K_a q/p)$
H_3O^+	3	2	−1.74	3.5×10^{11}	11.07	1.92
HOAc	1	2	4.56	3.2×10^{10}	10.51	−4.26
$H_2PO_4^-$	2	3	6.80	2.6×10^{10}	10.12	−6.62
H_2O	2	3	15.52	2.50×10^{6}[b]	6.10	−15.34

[a] $k_{HA}' = k_1 k_{HA}/(k_{-1} + k_0)$. [b] $k_{H_2O} = k_{HOCl}/[H_2O]$ ($[H_2O] = 55.5$ M).

Table VI. Comparison of Brønsted α Values

reacn	pK_a of the protonated Cl species	α	ref
$HA + OCl^- + I^-$	7.44	0.75	*a*
$HA + NH_2Cl + I^-$	1.5	0.65	*a*
$HA + NHCl_2 + I^-$	$\simeq -2.5$[a]	0.48	*a*
$HA + HOCl + I^-$	−4 to −3[b]	0.11	*c*
$HA + HOCl + Br^-$	−4 to −3[b]	0.27	*d*

[a] Reference 1. [b] Reference 27. [c] This work. [d] Reference 5.

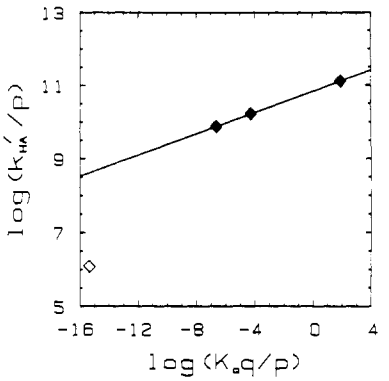

Figure 5. Brønsted plot for the general-acid-assisted reaction between HOCl and I^-. The point for k_{H_2O} (◇) was not used in the calculation of the linear parameters. The α value determined by linear regression is 0.11.

Comparisons to Previously Reported Kinetic Data. Table VI lists several general-acid-assisted reactions, the pK_a values for the protonated chlorine species, and the experimental Brønsted α values. For the four reactions listed that involve iodide and a reducible chlorine species, the α values decrease as the pK_a values decrease. The higher the α value, the greater the degree of proton transfer in the transition state. It follows that as the chlorine species becomes less basic it has less need for a proton in the transition state, and the α value decreases.

A direct comparison of the α values for the reaction of HOCl and HA with I^- and Br^- (Table VI) shows that the degree of proton transfer in the transition state (**1**) for the I^- reaction is less than in the reaction with Br^-. Iodide is a better nucleophile than bromide. Therefore, the I–Cl bond is more easily formed than the Br–Cl bond and requires less assistance from the proton of HA.

The rates of reaction of hypochlorous acid with halides can be compared (Table VII). The rates of the reactions between HOCl, H^+, and the halides are seen to follow a trend ($Cl^- < Br^- \ll I^-$).

(26) Espenson, J. H. *Chemical Kinetics and Reaction Mechanisms*; McGraw-Hill: New York, 1981; p 200.
(27) Arotski, J.; Symons, M. C. R. *Q. Rev., Chem. Soc.* **1962**, *16*, 282–297.
(28) Bell, R. P. *The Proton in Chemistry*, 2nd ed.; Cornell University Press: Ithaca, NY, 1973; p 198.

Table VII. Comparison of Reaction Rate Constants and the Free Energy Change for Reactions between Hypochlorous Acid and Halides

reacn	k, M^{-2} s^{-1}	$\Delta G°_{reacn}$, kJ mol^{-1}
$H^+ + HOCl + Cl^- \rightarrow Cl_2 + H_2O$	2.8×10^4 [a]	−19.0
$H^+ + HOCl + Br^- \rightarrow BrCl + H_2O$	1.3×10^6 [b]	−54[c]
$H^+ + HOCl + I^- \rightarrow ICl + H_2O$	3.5×10^{11} [d]	−120.3

[a] Margerum, D. W.; Gray, E. T., Jr.; Huffman, R. P. In *Organometals and Organometalloids, Occurrence and Fate in the Environment*; Brinckman, F. E., Bellama, J. M., Eds.; ACS Symposium Series 82; American Chemical Society: Washington, DC, 1978; pp 278–291. [b] Reference 5. [c] $\Delta G°$ for BrCl(g) used in calculation. [d] This work.

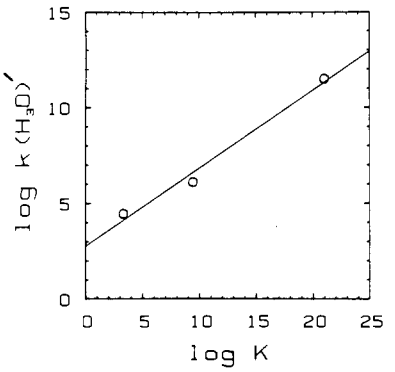

Figure 6. Linear free energy relationship for the reaction of HOCl and H^+ with Cl^-, Br^-, and I^-. Parameters obtained by least-squares linear regression: $\log k(H_3O)' = 2.8 + 0.41 \log K$.

Not only does the nucleophilicity of the halides increase along the series but $\Delta G°_{reacn}$ also becomes more favorable. These three sets of data have a linear free energy relationship as shown in Figure 6, which is a plot of eq 40 for the reaction $H^+ + HOCl + X^-$. It is interesting that the slope is 0.41 (±0.05), because a Marcus-type free energy correlation would predict a slope of 0.5 for an outer-sphere electron transfer[29] and a smaller slope for strong-overlap inner-sphere electron transfer.[30,31] Although we have a Cl^+-transfer reaction rather than a simple electron-transfer process, a similar correlation exists. Reactions of I_2 and Br_2 with various metal complexes, where the rate-determining step was postulated to be a combination of electron transfer and X–X bond cleavage (eq 41), also gave linear free energy relationships with slopes of 0.43 (±0.02) for I_2 and 0.45 (±0.07) for Br_2.[32]

$$\log k = 2.8 + 0.41 \log K \quad (40)$$

$$M^{II}LX_2 \rightarrow M^{III}L(X^-) + X^\bullet \quad (41)$$

Reaction of Trichloramine and Iodide. A major obstacle in the study of iodide reactions with NCl_3 is the presence of HOCl, which is normally present at 3–10% of the NCl_3 concentration. HOCl can interfere because the reactions of iodide with NCl_3 and HOCl are both on the PAF time scale and both lead to the formation of I_3^-. Our preliminary experiments showed that the reaction of NCl_3 and I^- is not as fast as that of HOCl and I^-. Also, even at relatively large I^- concentrations (2.5×10^{-3} M) the pseudo-first-order rate constants for $NCl_3 + I^-$ remain almost constant, with a maximum value of 13 900 s^{-1} (Table VIII).

As the PAF method employs integrating observation, the observed signal for two parallel reactions is a complex sum of both. We tested the effect of HOCl on the rate of the $NCl_3 + I^-$ reaction by determining the amount of HOCl present (by the Br^- method described in the Experimental Section) and by adding known quantities of HOCl until its concentration was greater than $[NCl_3]$

Table VIII. Kinetic Data for the Reaction of NCl_3 and I^-

$10^3[I^-]$, M	−log $[H^+]$	$10^6[HOCl]_T$, M	$10^{-3}k_r$, s^{-1}
0.404	2.01[a]	1.03	10.5 (5)
0.75	7.08[b]	≃1	12.6 (4)
0.965	6.99[b]	≃1	11.7 (2)
1.00	7.08[b]	≃1	13.2 (2)
1.50	7.09[b]	≃1	13.4 (2)
2.00	7.09[b]	≃1	13.9 (2)
2.50	7.07[b]	≃1	13.9 (2)
0.965	7.05[b]	0.748	12.0 (2)
0.965	7.04[b]	4.56	14.4 (4)
0.965	7.05[b]	8.36	15.8 (3)
0.965	7.05[b]	12.2	17.8 (3)
0.965	7.04[b]	16.1	19.7 (5)
			11.8 (2)[d]
0.965	4.54[c]	0.374	13.6 (5)
0.965	4.58[c]	3.39	17.0 (4)
0.965	4.56[c]	6.42	19.8 (5)
0.965	4.56[c]	9.42	25.0 (5)
0.965	4.55[c]	12.5	25.9 (8)
			13.3 (8)[d]

[a] $[NCl_3] = 1.0 \times 10^{-5}$ M; 0.973×10^{-3} M $HClO_4$. [b] $[NCl_3] = 1.1 \times 10^{-5}$ M; 0.01 M phosphate buffer. [c] $[NCl_3] = 1.1 \times 10^{-5}$ M; 0.01 M acetate buffer. [d] Extrapolated value.

(Table VIII). The k_r values increased significantly as [HOCl] increased, but the values extrapolated to [HOCl] = 0 are within the experimental errors of the values determined in experiments when no HOCl was added. This test was carried out in 0.965 $\times 10^{-3}$ M I^- in phosphate buffer at a −log $[H^+]$ value of 7.04, where the HOCl + I^- rate is much faster than the NCl_3 reaction with I^-. At 0.245×10^{-3} M I^- we found serious interference in the k_r values from the HOCl reaction with iodide.

If two fast reactions ($k > 5000$ s^{-1}) with the same product (I_3^-) are monitored with the PAF method, the slower reaction will give the dominant signal. A rearrangement of eq 12 is given in eq 42,

$$\Delta A_{obsd} = \frac{\Delta v}{b k_r} \Delta A_T \quad (42)$$

where ΔA_{obsd} is the absorbance range observed as the flow is accelerated from 3 to 12.5 m s^{-1}, Δv is the change in velocity (m s^{-1}), b is the reaction path length, and ΔA_T is the total absorbance change for the reaction ($A_0 - A_\infty$). If Δv and ΔA_T are held constant, ΔA_{obsd} is inversely proportional to the reaction rate constant. In our case, $NCl_3 + I^-$ is the slower reaction and accounts for the dominant component of the observed absorbance change.

There are three ways to avoid interference due to a faster reaction. First, choose a set of conditions where one reaction is too fast to be measured by the PAF method ($k_r \gg 200\,000$ s^{-1}). The contribution to ΔA_{obsd} will then be negligible. Second, the concentration of the reactant responsible for the faster reaction can be minimized so that the contribution to ΔA_T will be very small and ΔA_{obsd} is again negligible. Finally, the above two approaches can be combined. We have chosen this third approach to acquire reliable kinetic data for $NCl_3 + I^-$. The relationship in eq 43 follows from eq 42, and to keep the contribution of the undesired ΔA_{obsd}^{HOCl} to less than 1% of the signal the conditions in eq 44 must be met.

$$\frac{\Delta A_{obsd}^{NCl_3}}{\Delta A_{obsd}^{HOCl}} = \frac{\Delta A_T^{NCl_3}}{\Delta A_T^{HOCl}} \frac{k_r^{HOCl}}{k_r^{NCl_3}} \quad (43)$$

$$\frac{[NCl_3]}{[HOCl]} \frac{k_r^{HOCl}}{k_r^{NCl_3}} > 100 \quad (44)$$

A test for a −log $[H^+]$ dependence and a buffer dependence was made by addition of known amounts of HOCl and extrapolation of the k_r values to [HOCl] = 0 with an acetate buffer at a −log $[H^+]$ value of 4.56 and $[I^-] = 0.965 \times 10^{-3}$ M. The data are listed in Table VIII, and again the extrapolated value agrees well with the data obtained at a −log $[H^+]$ value of 6.99 in

(29) Marcus, R. A. *Annu. Rev. Phys. Chem.* **1964**, *15*, 155–196.
(30) Sutin, N.; Gordon, B. M. *J. Am. Chem. Soc.* **1961**, *83*, 70–73.
(31) Haim, A.; Sutin, N. *J. Am. Chem. Soc.* **1966**, *88*, 434–440.
(32) Woodruff, W. H.; Margerum, D. W. *Inorg. Chem.* **1974**, *13*, 2578–2585.

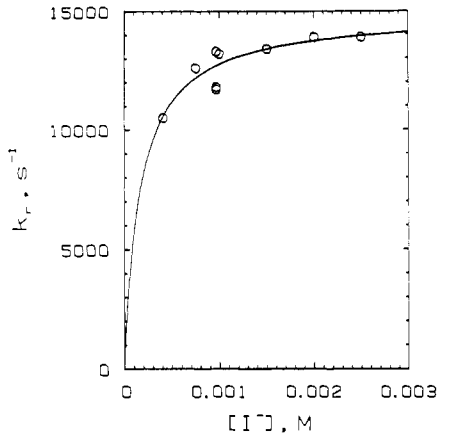

Figure 7. Plot of pseudo-first-order rate constants vs $[I^-]$, the excess reagent, for the reaction of NCl_3 and I^-. The curve was calculated through the use of eq 47, where $K_1 = 6 \times 10^3\ M^{-1}$ and $k_2 = 1.5 \times 10^4\ s^{-1}$.

phosphate buffer. This agreement means that there is no buffer dependence nor is there a hydrogen ion effect on this rate.

Examination of the rate constants for the HOCl + I^- reaction in acidic solutions shows that at $[H^+] = 10^{-2}$ M the rate is greater than 80000 s^{-1} with $[I^-] > 0.2 \times 10^{-3}$ M because of the H_3O^+-catalyzed path. Reliable data are obtained for the NCl_3 + I^- reaction in 0.01 M H^+, where eq 44 will be satisfied. At this acid concentration one of the products of the reaction, $NHCl_2$, will react with iodide in the time required to determine A_∞ for the reaction. The NH_2Cl formed by the second reaction will also react with iodide in this time span. Neither of these reactions is fast enough to interfere with the A_v measurement in the PAF observation tube. However, they do interfere with the A_∞ measurement because it is taken after several seconds. Hence, the only way to obtain $A_\infty^{NCl_3}$ is by calculation. The concentration of NCl_3 was determined with the molar absorptivity value of 195 M^{-1} cm^{-1}.[14] Previous determinations of the stoichiometry of the reaction of NCl_3 + I^- indicated that 0.8 I_2 molecule is formed for each NCl_3 consumed.[1] This assumption was used, along with the PAF path length and the molar absorptivity for I_3^- at 353 nm and the equilibrium constant in eq 6, to calculate $A_\infty^{NCl_3}$. Addition of this value to A_∞^{HOCl} gives A_∞^{reacn}, the true A_∞ value for the reaction of interest. The value calculated in this manner was used in the analysis of the data point at a −log $[H^+]$ value of 2.01 (Table VIII).

The mechanism we propose is described by eq 45, 46, 5, and 6, where an association complex, NCl_3I^-, is formed. We propose

$$NCl_3 + I^- \underset{}{\overset{K_1}{\rightleftharpoons}} NCl_3I^- \qquad (45)$$

$$H_2O + NCl_3I^- \xrightarrow{k_2} NHCl_2 + ICl + OH^- \qquad (46)$$

the interaction of I^- at one of the chlorine atoms because the expansion of the chlorine octet is more easily facilitated than expansion around nitrogen. The complex subsequently decomposes and I_3^- is eventually formed. Resolution of values for K_1 and k_2 was performed with eq 47, which is derived from the proposed

$$k_r = [(K_1[I^-])/(1 + K_1[I^-])]k_2 \qquad (47)$$

mechanism. The fit of the model to the data can be seen in Figure 7. A simplex optimization procedure[24,25] was employed, and the value for K_1 was found to be 6 (±2) × 10^3 M^{-1}, and the value for k_2 is 1.5 (±0.1) × 10^4 s^{-1}.

The formation of an association complex of the form NCl_3I^- is only one way to arrive at a mechanism that follows saturation kinetics, but two other possibilities can easily be eliminated. The rapid preequilibrium cannot be due to the hydrolysis of NCl_3 (eq 48), because the rate of the forward reaction is extremely slow

$$NCl_3 + H_2O \rightleftarrows NHCl_2 + HOCl \qquad (48)$$

(1.6×10^{-6} s^{-1}).[9] The equilibrium constant[9] has been reported to be 6.25×10^{-9} M, which is much too small to play an important role in the present mechanism. The negligible hydrolysis rate constant for NCl_3 justifies the extrapolation of the k_r value to zero in Figure 7, where $[I^-] = 0$.

Another possibility is that the incoming I^- attacks NCl_3 at the nitrogen, as described in eq 49. The reaction of NCl_3 + I^- was

$$NCl_3 + I^- \rightleftarrows NCl_2I + Cl^- \qquad (49)$$

followed in the presence of 0.5 M Cl^-, where the product is a mixture of I_3^- and I_2Cl^-, and the rate at $[I^-] = 1.00 \times 10^{-3}$ M and −log $[H^+]$ = 7.05 was 13.3 (±0.3) × 10^3 s^{-1}, in excellent agreement with other values at similar conditions with no excess Cl^- present, as seen in Table VIII. The presence of excess Cl^- would have slowed the rate considerably had the equilibrium in eq 49 been active.

Still, the method of choice would be to follow directly the loss of NCl_3 or, in the UV region, of NCl_3I^-. The reaction could be monitored at different wavelengths, but since the spectrum of NCl_3I^- is unknown, we do not know what the observed absorbance change will mean. In addition, the absorbance of I^- at low wavelengths and of I_3^- at longer wavelengths would interfere.

The fact that the reaction of NCl_3 and I^- does not follow the general-acid-assisted mechanism indicates that NCl_3 is a very poor base. The protonation constant of NCl_3 has not been determined, but it must be less than the value estimated for $NHCl_2$, which is −2.5.[1] Neither NCl_3 nor NCl_3I^- appears to accept a proton until ICl dissociates, which leaves NCl_2^-, an excellent base. The α value for this reaction is zero, because a proton is not involved in the transition state.

Conclusions

In the reaction of iodide with HOCl and with NCl_3, kinetic saturation effects lead to two postulated intermediates, $HOClI^-$ and NCl_3I^-, with association constants of 220 and 6000 M^{-1}, respectively. The larger value for I^- association with NCl_3 is consistent with the greater polarizability of this molecule compared to that of the HOCl molecule. The rate of loss of ICl from $HOClI^-$ is 60 times greater than the corresponding reaction of NCl_3I^-. The latter reaction does not appear to be assisted by acid even in 10^{-2} M $HClO_4$, while the breakup of $HOClI^-$ is strongly acid-assisted. There is still much to learn about these fast reactions. The PAF method permits the first views of their reaction pathways. We have attempted to present some of the abilities and limitations of the PAF method when series and parallel reactions are encountered.

Acknowledgment. This work was supported by National Science Foundation Grants CHE-8616666 and CHE-8720318.

Registry No. I^-, 20461-54-5; HOCl, 7790-92-3; NCl_3, 10025-85-1.